

# *Results from a Lunar Laser Communication Experiment between NASA's LADEE Satellite and ESA's Optical Ground Station*

Zoran Sodnik, Hans Smit, Marc Sans  
European Space Research and Technology Centre  
European Space Agency  
Noordwijk, The Netherlands  
zoran.sodnik@esa.int

Dirk Giggenbach, Peter Becker,  
Ramon Mata-Calvo, Christian Fuchs  
Institute of Communications and Navigation (IKN)  
German Aerospace Center (DLR)  
Wessling, Germany

Igor Zayer, Marco Lanucara, Klaus-Jürgen Schulz  
European Space Operation Centre  
European Space Agency  
Darmstadt, Germany

Johannes Widmer, Felix Arnold,  
Martin Mosberger  
RUAG Space Zürich AG  
Zürich, Switzerland

Angel Alonso, Iciar Montilla  
Instituto de Astrofísica de Canarias (IAC)  
La Laguna, Tenerife, Spain

**Abstract**—ESA's optical ground station (OGS) participated in the Lunar Laser Communication Demonstration (LLCD) with the Laser Communication Space Terminal (LLST) onboard NASA's Lunar Atmosphere and Dust Environmental Explorer (LADEE) satellite. The experiment demonstrated the capabilities of optical communication and of inter-agency cross-support for optical communication links. The OGS experimental campaign, which started on October 26 and lasted until November 20, consisted of four days of bidirectional link sessions followed by three days of no operation. Each individual link session lasted approximately 20 minutes and was repeated after two hours. Despite non optimal weather conditions multiple link sessions were performed. The paper describes the design of the transmit laser and data generation system as well as the receiver system. A special chapter is dedicated to lessons learned from transmitter/receiver alignment problems, which prevented the demonstration of data uplink and ranging from the OGS. Several possibilities to solve the alignment problem are discussed and the finally implemented solution is described.

**Keywords**—Free-space optical communication systems; laser communication terminal; transmitter diversity; OGS; LLCD; LADEE

## I. INTRODUCTION

Laser communication technology developments started in the European Space Agency (ESA) in the mid of the 1970s and have continued ever since. In 2001 the world-first optical inter-satellite communication link was demonstrated (SILEX) between the ARTEMIS data-relay satellite in geostationary orbit (GEO) and the SPOT-4 Earth observation satellite in low earth orbit (LEO) [1][2][3][4][5]. The Japanese space agency JAXA joined in the inter-satellite communication experiment

with its OICETS satellite in LEO and the French department of defense demonstrated a bidirectional communication link from an aircraft [6][7][8].

SILEX was an important milestone demonstrating that the stringent pointing and tracking accuracies required for laser communication can be mastered in space; although the technology used for SILEX was not able to compete with state of the art radio communication technology in terms of mass (160 kg) and data rate (50 Mbps).

A second generation of Laser Communication Terminals (LCT) with a mass of 35 kg has subsequently been developed by the German Space Agency (DLR) and were launched in 2007 on two LEO spacecraft (TerraSAR-X and NFIRE). Inter-satellite communication links at 5.6 Gbps over a maximum distance of 6,000 km have been demonstrated [9].

The European Data Relay Satellite (EDRS) system will utilize a modified LCT version for its LEO to GEO inter-satellite communications links, which will have a mass of 54 kg and enable data rates of 1.8 Gbps over 45,000 km. An artist's impression of the EDRS system is shown in Fig. 1. EDRS will provide an increase in data availability and use a coherent transmission and reception technology based on a wavelength of 1064 nm.

As an independent check-out facility for LCTs in space, ESA developed the Optical Ground Station (OGS) at the Observatorio del Teide (OT) on Tenerife, Spain. The OGS is used to commission and test laser communication terminals, such as those on the ARTEMIS, OICETS, TerraSAR-X and NFIRE satellites. It is now being prepared to test the LCTs onboard the Alphasat, EDRS-A and EDRS-C satellites.



Fig. 1. Artist's impression of two EDRS satellites in GEO servicing Sentinel 1a and 2a in LEO as well as ESA's OGS

The first European lunar satellite, SMART-1, was launched in 2005 into an elliptical geostationary transfer orbit (GTO) and used electrical propulsion to periodically increase its apogee altitude until caught by lunar gravity. Laser link experiments were performed when the electric propulsion was switched off and SMART-1 was able to turn its camera towards Earth and valuable open-loop pointing acquisition and tracking procedures were exercised.

## II. BACKGROUND

NASA's Lunar Atmosphere and Dust Environmental Explorer (LADEE) satellite's main mission goal is to study the pristine state of the lunar atmosphere and dust environment. It carries several scientific instruments [11] and in addition a technology demonstration payload, namely the Lunar Laser Space Terminal (LLST) for the demonstration of high speed (up to 622 Mbps downlink and up to 19 Mbps uplink) optical communication with a ground station.

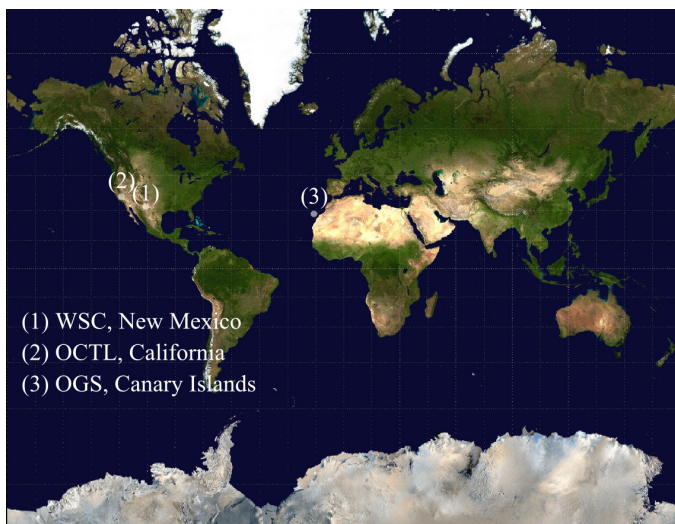


Fig. 2. Locations of the three ground station participating in LLCD

The Lunar Laser Communication Demonstration (LLCD) is being undertaken by MIT Lincoln Laboratory, where the Lunar Laser Space Terminal (LLST) was built. In addition a Lunar Laser Ground Terminal (LLGT) was developed and eventually moved to the White Sands Complex (WSC) in New Mexico. The Jet Propulsion Laboratory (JPL) and the European Space Agency ESA (ESA) were invited to participate with their own specific ground facilities, namely from the Optical Communication Telescope Laboratory (OCTL) on Table Mountain, California, and from the Optical Ground Station (OGS) in Tenerife. The three ground station locations are shown in Fig. 2.

The LADEE spacecraft was launched on September 7<sup>th</sup>, 2013 and the LLCD, not being the primary mission target of LADEE was performed during the satellite's commissioning and testing phase upon its arrival in lunar orbit. Operations from the OGS started on October 26, 2013. An artist's impression of the laser communication link is shown in Fig. 3.

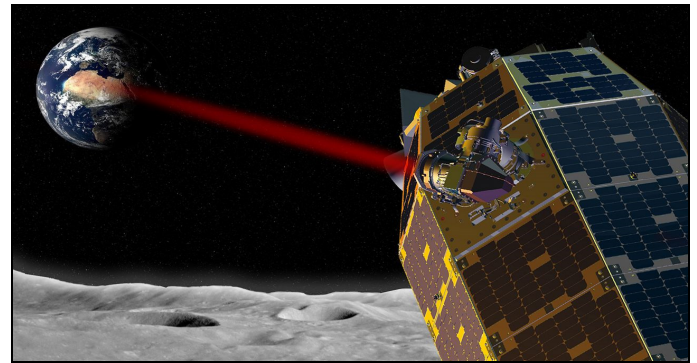


Fig. 3. Artist's impression of the LLST onboard the LADEE spacecraft transmitting towards Earth

The campaign was organized by four days of operations, followed by three days of no operation. During this period, the satellite was in a ~2 hour lunar orbit at an altitude of about 200 km and operations were limited in duration to 15-20 minutes per orbital pass due to thermal and power limitations onboard the spacecraft.

TABLE I. PARAMETERS OF THE LASER COMMUNICATION LINK BETWEEN LLST AND THE OGS

Parameter	Description	Value
Range	Lunar distance	362570 – 405410 km
Wavelength	Downlink	1550.12 ± 0.1 nm
	Uplink Communication	1558.17 ± 0.02 nm
	Uplink Acquisition	1567.95 ± 0.1 nm
Modulation Format	Downlink	16-PPM
	Uplink	4-PPM
Data Rate	Downlink (to OGS)	38.55 Mbps
	Uplink (from OGS)	19.28 Mbps
Downlink Irradiance	Specified at border of atmosphere	0.17 - 1.7 nW/m <sup>2</sup>
Uplink Irradiance	Specified at LADEE spacecraft	36 – 63 nW/m <sup>2</sup>

A summary of the LLCD operational parameters for the communication link with the OGS are shown in Table I. While the MIT Lincoln Lab station demonstrated downlink data rates up to 622 Mbps using a very sophisticated detector technology (cryogenically cooled nano-wire detectors), the downlink data rates to the ESA OGS were limited to 38 Mbps using commercial photon counting detectors (Hamamatsu) and – for test purposes - a Mercury Cadmium Telluride (MCT) avalanche photo-detector from the French company Leti/LIR.

### III. THE ESA OPTICAL GROUND STATION (OGS)

The European Space Agency's Optical Ground Station (OGS) is located at the Observatorio del Teide (OT) in the Canary Islands (Tenerife, Spain). Its main purpose is to check out and commission laser communication terminals onboard orbiting spacecraft. The OGS is also used for Space Debris, asteroid and near Earth object (NEO) detection and for standard astronomical observations.



Fig. 4. The Observatorio del Teide site in Tenerife, Canary Islands, Spain



Fig. 5. OGS building with mount Teide in background

The Canary island archipelago also offers the opportunity to perform inter-island experiments. From the island of La Palma, at a distance of 142 km, novel laser communications systems and quantum communications (entanglement and

teleportation) experiments are being performed. The Observatorio del Teide site is shown in Fig. 4.

The OGS building shown in Fig. 5 houses a 1-meter Zeiss telescope using an English mount (where the hour axis is supported by a North and a South pillar).

The telescope has two optical configurations; either a Cassegrain or a Coudé configuration can be selected. The Coudé configuration was not used for LLCD. Fig. 6 shows the telescope on one side of the hour axis, with a counter weight on the other. The telescope aperture is surrounded by a dew cap (triangular flaps around the telescope aperture), which is closed in the picture. The hour axis is parallel to Earth's axis and is therefore tilted by 28.3 degrees, which corresponds to the latitude of the OGS location.

TABLE II. LOCATION OF THE OGS AND ITS MAIN TELESCOPE PARAMETERS

Parameter	Value
Geographic longitude	16° 30' 36.36" West
Geographic latitude	28° 17' 58.29" North
Altitude above sea level	2393 m
Telescope aperture diameter	1016 mm
Telescope focal length	13300 mm
Acquisition and tracking camera (ATC) pixel size	20 $\mu\text{m}$ x 20 $\mu\text{m}$
Photo-detector multimode fiber core diameter	200 $\mu\text{m}$



Fig. 6. The English mount of the 1 meter Zeiss telescope

#### A. Transmitter design

The transmitter design is bi-static and was driven by the assumption that only a geometrical separation between the transmitters and the receiver could prevent cross-talk. It was anticipated that with the extremely high dynamic range of >100 dB between the transmitted and received signals it would not be possible to develop a mono-static design. However, the OCTL design from JPL demonstrated that a mono-static design is feasible.

As shown in Fig. 7 three individual transmit apertures with 40 mm diameter are arranged around the 1 meter telescope receive aperture. One of the three transmit apertures is covered by a large aperture (120 mm diameter) corner cube retro-reflector (CCRR), which send the transmitted light back into the receiver for alignment purposes. This alignment procedure is performed for each of the three transmitters after which the CCRR is removed.

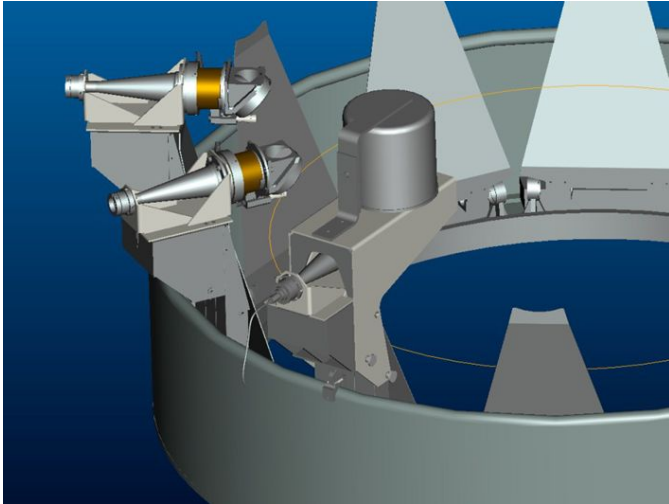


Fig. 7. Three transmitter systems as attached to the telescope aperture. The “cap” on one of the three transmitters is a corner-cube retro-reflector (CCRR) used to align the transmit beam direction of each of the three transmitters with the receiver. The CCRR is removed after alignment

The three transmitter apertures are driven from three fiber amplifiers (3SPhotonics/Manlight) producing 40 Watts of optical output power each. The fiber amplifiers, attached to the side of the telescope tube, are driven from six seed lasers, three for acquisition and three for communication purposes. The communication lasers are followed by data modulators (Photline).

Three transmitters are used to:

- Increase the transmit power, because the most powerful commercial fiber amplifier delivers 40 Watts average power max.
- Decrease the atmospherically induced fading (scintillation) of the uplink beam. The three transmit beams are geometrically separated and therefore pass different sections of the atmosphere. The speckle pattern created in the far field is therefore different for each beam. The fact that the wavelength of each beam is slightly different prevents interference and generates a more homogeneous far-field pattern.

#### 1) Acquisition laser system

For detection by the LLST, the acquisition signal requires a 50% duty cycle intensity modulation at 1 kHz. The initially design implemented was to drive the seed laser current with a corresponding modulation signal.

This approach failed for two reasons:

- The low frequency of the seed laser modulation current caused a laser diode temperature modulation, which lead to laser line-width spreading beyond the spectral width of the LLST input filter.
- The OGS fiber amplifiers were not able to cope with 1 kHz amplitude modulated input signal. As a matter of fact the internal optical isolator of one fiber amplifier (3SPhotonics/Manlight) was destroyed during testing with 1 kHz input modulation.

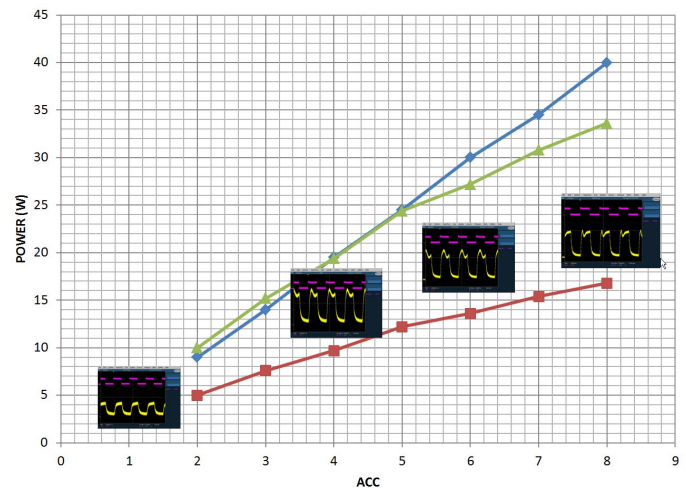


Fig. 8. The graph shows the fiber laser output power versus the drive current (Amperes) of the third modulator stage. The blue curve represents the unmodulated output power, the red curve the 1kHz modulated output power and the green curve is a multiplication of the red curve by two. Modulation more than halves the output power due to ringing

TABLE III. ACQUISITION LINK MARGIN FOR THE OGS UPLINK BEAM

Parameter	Initial Acquisition Value	Stable Tracking Value
Tx average power (3 x 40 W)	50.8 dBm	50.8 dBm
Tx modulation penalty caused by the 50% duty cycle, 1 kHz intensity modulation (see Figure 8)	-3.5 dB	-3.5 dB
Tx antenna gain (40 mm $1/e^2$ diameter)	98.1 dB	98.1 dB
Tx transmission loss	-0.4 dB	-0.4 dB
Tx Strehl loss	-1.3 dB	-1.3 dB
Atmospheric transmission loss	-1.5 dB	-1.5 dB
Scanning pattern loss (6 arcsec step width)	-3.0 dB	0.0 dB
Free space loss (400000 km)	-310.1 dB	-310.1 dB
Rx antenna gain per unit area	127.1 dB/m <sup>2</sup>	127.1 dB/m <sup>2</sup>
Irradiance at LLST	-43.8 dB/m <sup>2</sup>	-40.8 dB/m <sup>2</sup>
Required acquisition signal irradiance	-54.4 dB/m <sup>2</sup>	-44.4 dB/m <sup>2</sup>
<b>Uplink acquisition margin</b>	<b>10.6 dB</b>	<b>3.6 dB</b>

The solution found was to modulate the pump diodes of the third (and last) amplification stage of the fiber amplifiers with a 1 kHz modulation signal. This caused the modulation extinction ratio to drop to 10 dB (3 dB below specification) but proved sufficient to acquire the LLST. The company 3SPhotonics/Manlight implemented this additional feature into all three amplifiers in a very short time and the laser amplifier output power versus the drive current is shown in Fig.8.

The link margin for the acquisition uplink signal is given in Table III. The three transmitters emit 40 Watts each, but the modulation penalty is taken into account. The scanning pattern loss only applies during initial acquisition because the OGS scans its transmit beams such that the irradiance drop in the far-field pattern does not exceed 3dB.

## 2) Communication laser system

As the uplink modulation format for communication is 4-PPM with a pulse width of 3.2 nanoseconds, the pulse delay through the three transmitters must be identical to fractions of a nanosecond such that all three transmitters operate simultaneously.

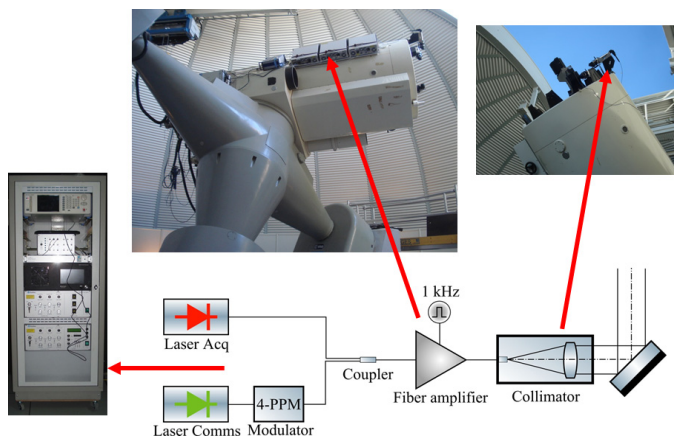


Fig. 9. Transmitter system block diagram and implementation on telescope

However, the seed lasers are located in a thermally stabilized Coudé room and connected to the fiber amplifiers via 30 meter long single-mode fibers.

TABLE IV. COMMUNICATION LINK MARGIN FOR THE OGS UPLINK BEAM

Parameter	Value
Transmitted average power (3 x 40 Watts)	50.8 dBm
Tx antenna gain (40 mm, $1/e^2$ diameter)	98.1 dB
Tx transmission loss (0.91)	-0.4 dB
Tx Strehl loss:	-1.3 dB
Atmospheric transmission loss (0.71)	-1.5 dB
Free space loss (400000 km)	-310.1 dB
Rx antenna gain per unit area	127.1 dB/m <sup>2</sup>
Irradiance at LLST	-37.3 dB/m <sup>2</sup>
Required comms irradiance at LLST:	-42.0 dB/m <sup>2</sup>
<b>Uplink communication margin</b>	<b>4.7 dB</b>

As it turned out the largest contributor to the differential pulse delay through the system was the internal active fibers lengths of the three fiber amplifiers. Using fast photo-detectors and an oscilloscope it was possible to measure the individual pulse delay and up to 6 meters in cable length difference were measured. This delay was then compensated by electrically driving the three laser modulators using coax-cables of different length. The individual components of the transmitter systems together with a block diagram are shown in Fig. 9. The link margin for the communication uplink signal is given in Table IV.

## B. Receiver design

Due to the weak signal irradiance from LLST in lunar distance, the OGS optical receiver design is driven by the need to minimize transmission losses. The receiver system is therefore installed in the Cassegrain focus, where the least number of optical elements in the telescope are present (2 reflective surfaces, namely primary and secondary mirror).

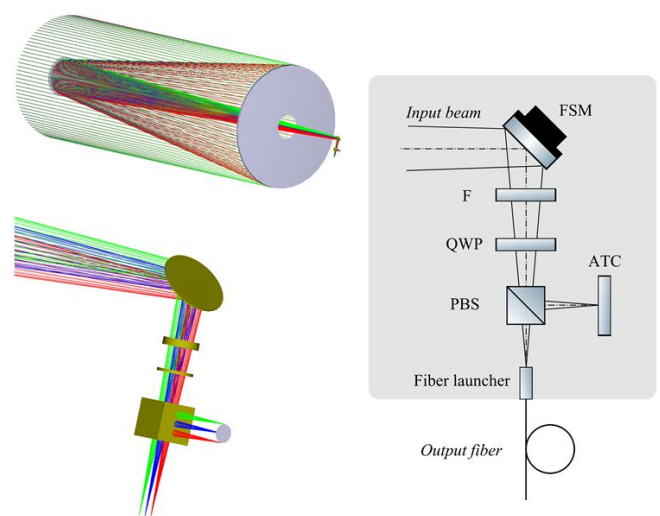


Fig. 10. Receiver optical ray-tracing (left) and schematic layout (right). The acronyms are fine steering mirror (FSM), filter (F), quarter wave plate (QWP) polarizing beam splitter (PBS) and acquisition and tracking camera (ACT)

The focal plane instrumentation is schematically shown in Fig. 10 and its real implementation in Fig. 11. It does not include a collimator but routes the converging beam from the telescope via a filter wheel (where two narrow band-pass interference filters can be selected with 2.4 nm and 5 nm FWHM bandwidth), a tip/tilt fast steering mirror (FSM) to adjust the point ahead angle (PAA), a computer-rotated quarter-wave plate (QWP) and a polarizing beam splitter (PBS) to the acquisition and tracking camera (ACT) and the receiver fiber. As the receive beam is circularly polarized, the QWP and PBS pair enable continuous adjustment of power ratio between the ACT and the detector fiber. During the initial satellite acquisition all power is directed towards ACT, until irradiance increases. Then the optical power towards the ACT is reduced (to the minimum level required to perform telescope pointing corrections) in favor of providing maximum power to the detector fiber.

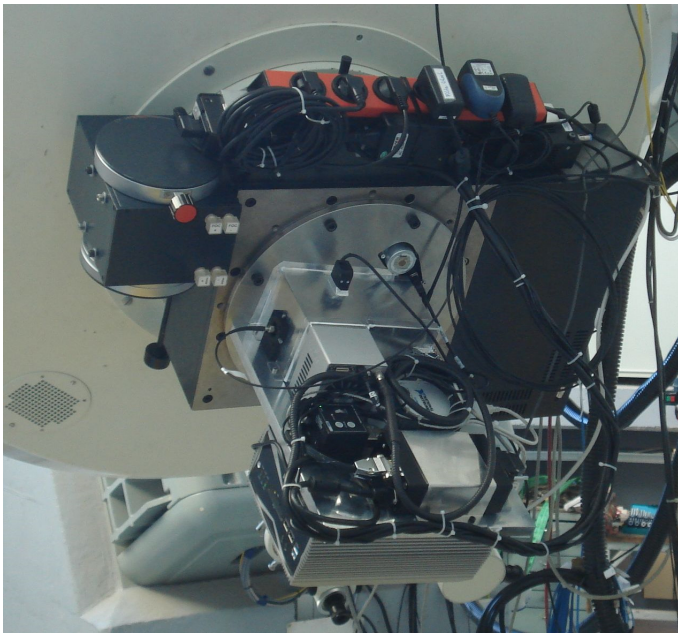


Fig. 11. The focal plane instrumentation attached to the Cassegrain focus

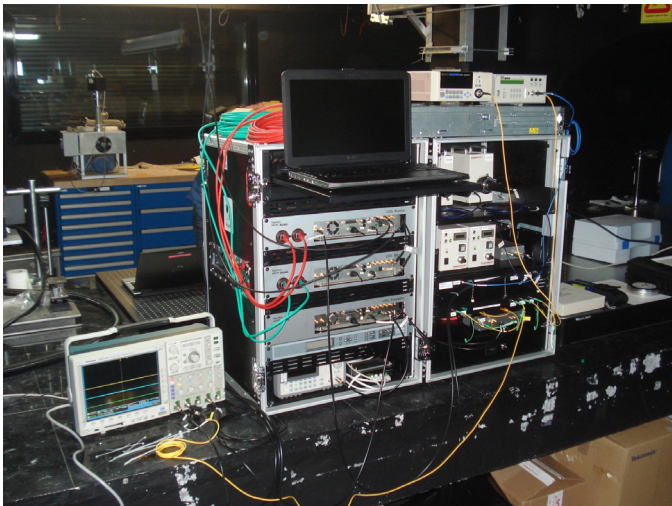


Fig. 12. The multi-mode fiber-coupled detection, demodulation and storage system developed by RUAG Space. It is located in the thermally stabilized Coudé laboratory

The design did not include a fast tip/tilt compensation loop, because a data receiver's field of view (FOV) of  $15 \mu\text{rad}$  was assumed to cover all possible angle of arrival fluctuations. Unfortunately, this turned out to be incorrect will be improved for the next LLCD campaign in April 2014.

The detection, demodulation and data storage system shown in Fig. 12 was developed by RUAG Space and is installed in the Coudé laboratory of the OGS. It is connected to the focal plane instrumentation at the telescope via a  $200 \mu\text{m}$  core diameter multimode fiber and its location provides a temperature stabilized environment.

The downlink budget is given in Table V. For the acquisition and tracking camera (ATC) it takes the minimum irradiance specified from LLST (at the start of acquisition) at

the top of the atmosphere and evaluates the received power per ATC pixel. This is put in relation with the expected background noise sources from the blue sky brightness (at daytime) and from the sun-illuminated lunar surface, taking an ATC pixel size or  $20 \mu\text{m} \times 20 \mu\text{m}$  and a seeing diameter of  $1 \text{ arcsec} = 65 \mu\text{m}$  into consideration.

After initial acquisition of the LLST signal, the tracking phase starts and the signal strength increases by a factor of 10. In the right column of Table V the received power is given for the OGS data detector, which is coupled via a 30 meter long graded index multimode fiber to the focal plane instrumentation. The assumption is made that the power splitting ration between the ACT and the fiber is set such that 90% reach the fiber and 10% the ACT. As the fiber core diameter is  $200 \mu\text{m}$  (which corresponds to  $3 \text{ arcsec}$ ), no coupling loss is assumed.

TABLE V. COMMUNICATION LINK MARGIN FOR THE LLST TO OGS DOWNLINK

Parameter	ATC Value	Detector Value
Irradiance from LLST at the border of the atmosphere	-67.7 dBm/m <sup>2</sup>	-57.7 dBm/m <sup>2</sup>
Atmospheric transmission loss	-1.5 dB	-1.5 dB
Telescope transmission loss incl. filter:	-3.2 dB	-3.2 dB
Seeing loss (pixel/1arcsec); beam splitting loss ATC/MMF (0.9) and MMF insertion loss (0.8)	-9.1 dB	-1.4 dB
Rx antenna loss factor per unit area ( $0.72 \text{ m}^2$ )	-1.4 dB/m <sup>2</sup>	-1.4 dB/m <sup>2</sup>
Received power	-82.9 dBm	-65.2 dBm
Lunar irradiance background	-111.8dBm	-92.8 dBm
Blue sky brightness	-97.7 dBm	78.7 dBm

#### IV. LLCD OPERATIONS AND PROBLEMS ENCOUNTERED

##### A. Transmitter misalignment

During the installation of the three transmitter systems in the OGS it became clear that it was not possible to perform a transmitter beam pointing alignment with the precision required. The bi-static installation of the transmitters and the receiver caused a varying deflection, dependent on the pointing direction of the telescope. The magnitude of the deflection proved to be larger than the divergence angle of the transmit beams. Unfortunately, active transmitter pointing control had not been foreseen and to minimize the pointing error it was necessary to perform the transmitter alignment (to the receiver by attaching the CCRR) with the telescope placed in the pointing direction, where LLCD experiment would take place. This meant that reaching of all three transmitter apertures would be very difficult and in some telescope pointing directions impossible. Thus LLCD operation from the OGS had to be cancelled when the telescope had to be pointed in western direction and at high elevation angles.

A second and even more important problem was differential misalignment between the three transmitters. Even during the 20 minutes of LLCD experiments per communication link session, The misalignment of the three transmitter beams with respect to the receiver was beyond acceptable limits. The following strategy was followed:

- Measure and store the Tx/Rx deflection of one of the three transmitter beams (with the acquisition and tracking camera by attachment of the corner-cube retro-reflector) and move the telescope along the satellite trajectory.
- Correct the measured deflection of that transmitter during the satellite pass using the fine steering mirror (FSM).
- Move the telescope to the central position of the satellite trajectory and minimize the pointing error of the two other transmitter beams.

In this way the alignment problem of one transmit beam should have been removed. As for the other two transmitters, their pointing error should have been compensated at the half way point of the satellite pass and their maximum pointing error halved. However, due to the experimental nature of LLCD, the start time of the laser communication experiment was not fixed and could be delayed by up to 15 minutes due to unforeseen events, such as the duration of the LLST heat-up process or the up-loading of the system parameter and the pointing data.

This resulted in a drift of the alignment of the transmitters and only one laser transmitter was effectively in use during the LLST laser links, with the other two not contributing to the uplink budget. A single transmitter (instead of three) results in a penalty of -4.8 dB and when applying this to the link margin in Table III it becomes clear that stable tracking from LLST was not possible as the link margin became negative (-1.2 dB).

Thanks to the robust LLST design with additional margin implemented, stable tracking was possible for sufficiently long durations of time to successfully retrieve error-free data from the LLST in mode 5 at a data rate of 38.55 Mbps. The results of the data reception are presented in [15].

### B. Transmitter beam quality

A third problem materialized during the telescope alignment, namely a distorted point spread function (PSF) of the transmit beams as observed in the focal plane of the telescope by the ATC. The PSF showed Coma and this fact was confirmed when – for testing purposes – the OGS transmitted a single beam only, scanning the far field and the LLST measuring the irradiance. The correspondence between the PSF and far-field-pattern (FFP) is quite striking as shown in Fig. 13.

Caused by the transmitter problems the switch-over from acquisition to uplink communication was not possible and the uplink and ranging electronics, developed by the Danish company Axcon, could not be tested.

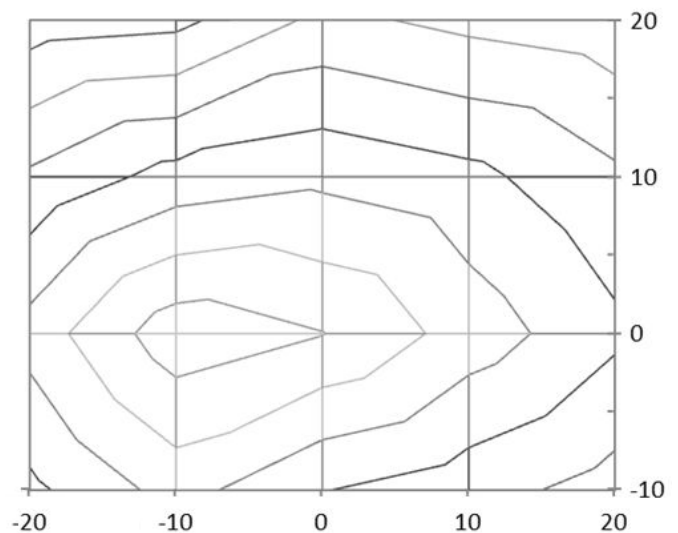
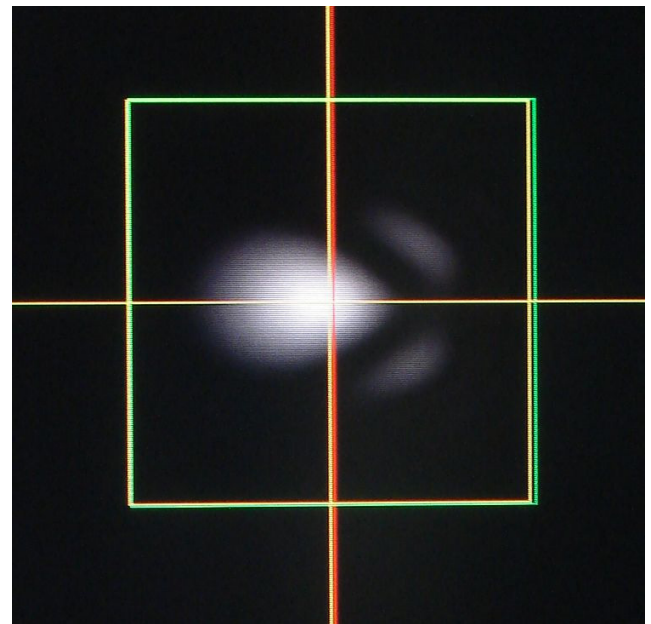


Fig. 13. The point spread function of one beam measured in the focal plane by the ATC during beam alignment with a corner-cube retro-reflector attached (top) and the far-field-pattern (FFP) measured by LLST during a raster type scan of the OGS transmitter (bottom)

### C. Receiver tracking-loop implementation

The design of the focal plane instrumentation does not foresee a fast tracking loop which keeps the received beam from LLST on the center of the receiver fiber. The reasoning behind was the relative large field-of-view (FOV) of the graded index multimode fiber of  $200\ \mu\text{m} = 3\ \text{arcsec}$ , which was assumed to cover beam spreading and image motion caused by atmospheric turbulence and telescope tracking errors. This assumption however turned out to be incorrect and the telescope had to be realigned multiple times to keep the spot on the fiber.

## V. IMPROVEMENTS AND OUTLOOK

NASA indicated the possibility to provide another week of laser communication experiments with LLST after finalizing the LADEE science phase. The latest information is that another test campaign may become possible by end of March 2014. ESA placed a contract with the Swiss company Synopta to improve the transmitter design.

The proposed solution, shown in Fig. 14, is to actively control the alignment of all three beams, by placing a laser beacon into the focal plane of the telescope. A single mode laser operating at a wavelength of 980 nm is coupled via a dichroic beam-splitter cube (to avoid aberrations in a diverging beam) into the telescope path (in front of the filter wheel) and shines its beam out of the 1-meter aperture of the telescope.

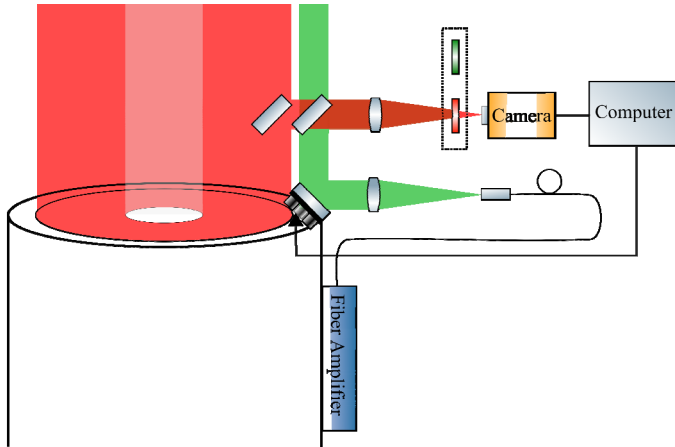


Fig. 14. A beacon beam (red) originating from the focal plane and shining out of the telescope tube is sampled at the rim of the aperture by a mirror and superimposed with the transmit beam (green) on an anti-reflection coated glass plate. Mutual alignment is achieved by measuring the angular direction of both beams successively through two interference filters with an InGaAs camera. A computer controlled tip/tilt mirror ensures that both beams stay co-aligned whatever the telescope position/pointing direction. This set-up is repeated three times for each transmitter

A 1550 nm filter located in the filter wheel prevents detection of the 980 nm beam by the ATC. The beacon beam carries the angular information about the center of the Acquisition and Tracking Camera (ATC), but is influenced (deflected) by telescope tube deformations, which vary with changing telescope pointing directions. Each transmitter will be equipped with its own InGaAs camera, which successively (using a rotating interference filter wheel) picks up a small attenuated portion of the transmit beam and the beacon beam from out of the telescope using a mirror and an anti-reflection coated plate. The camera is read out by a computer, which constantly determines the angular mismatch between the transmit beam (1558 nm or 1568 nm) and the beacon beam (980 nm) and adjusts the transmit beam direction via piezo-controlled micrometers such that both point in the same direction. In this way the transmit/receive beam alignment should stay constant in any telescope pointing direction.

The coma of the transmitter beams has been identified as a miss-alignment problem and will be fixed.

A fast and automatic tracking loop will be implemented, which keeps the received beam from the LLST centered on the detector multimode fiber. The fine steering mirror (FSM) located in the focal plane assembly and currently used to adjust the point ahead angle (PAA) will perform fast closed loop tracking with beam offset information provided by the acquisition and tracking (ACT) camera. This, together with the telescope tracking system will form two nested tracking loops with different response times, because also the point-ahead angle (PAA) needs to be maintained. The high frequency tracking loop around the nominal PAA position will be checked for low frequency angular drifts (offsets) from the PAA position and those offsets will be sent at low frequency to the telescope tracking system for removal.

In addition (as backup solution) a transmitter system has developed as shown in Fig. 15, which combines all three beams and transmits them from a single aperture. To do so it uses two mirrors aligned at 90 degrees that deflect the 5 mm diameter collimated beams from two fiber amplifier collimators in the direction of a third fiber amplifier collimator. The beam directions of all collimators can be aligned with micrometers and they are followed by a Galilean magnifying telescope which increases the beam diameter of each beam to 35 mm.

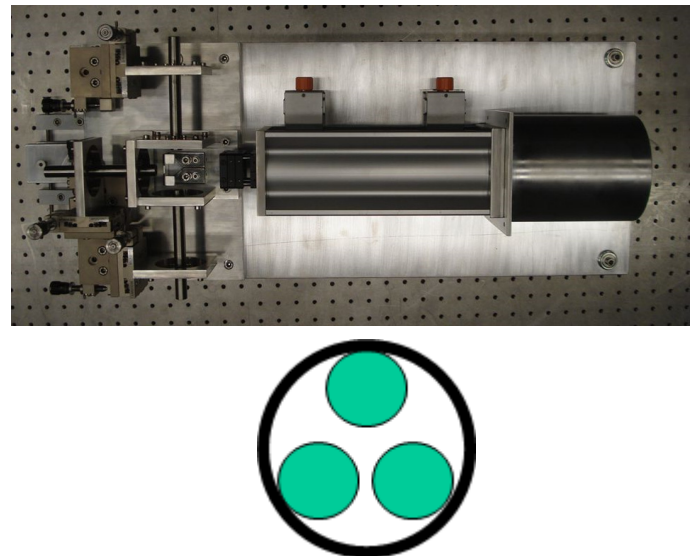


Fig. 15. Alternative transmitter system combining three beams from fiber amplifier collimators (shown on the top left) and magnifying them by a Galilean system (top right). The arrangement of the beams from the three fiber amplifier collimators in the aperture on the beam combining system is shown below. The three 35mm diameter beams (green) are shown in relation with the 100 mm Galilean beam expander aperture (black)

The alternative transmitter system will be attached to the side of the 1 meter telescope tube.

## VI. CONCLUSIONS

ESA's optical ground station successfully performed acquisition, tracking and data reception from the Lunar Laser Space Terminal onboard the LADEE satellite during the LLCD measurement campaign in October/November 2013.



However, a couple of technical problems prevented the demonstration of data uplink and ranging. The proposed solution of those problems has been described and is being implemented in the OGS. It is hoped that the full performance of the OGS including a demonstration of data uplink and ranging will become possible in the follow-up Lunar Laser Communication Demonstration (LLCD) campaign scheduled for early April 2014.

#### ACKNOWLEDGMENT

The authors would like to thank John Rush, Don Boroson, Donald Cornwell, Joseph Kovalik from NASA, Robert Daddato from ESOC, Reinhard Czichy from Synopta, Anders Enggaard and Thorben Vendt Hansen from Axcon, Sebastien Grot from 3SPhotonics/Manlight and Herve Gouraud from Photline for support and helpful discussions.

#### REFERENCES

- [1] Tolker-Nielsen T., Oppenhauser G., "In-orbit test result of an operational optical inter satellite link between ARTEMIS and SPOT4, SILEX". Proc. SPIE, 2002, vol. 4635, pp.1–15.
- [2] Alonso A, Reyes M, Sodnik Z., "Performance of satellite-to-ground communications link between ARTEMIS and the Optical Ground Station", Proc. SPIE, 2004, vol. 5572, p. 372.
- [3] Romba J, Sodnik Z, Reyes M, Alonso A, Bird A, "ESA's Bidirectional Space-to-Ground Laser Communication Experiments". Proc. SPIE, 2004, vol. 5550, pp. 287- 298.
- [4] Reyes M, Alonso A, Chueca S, Fuensalida J, Sodnik Z, Cessa V, Bird A, "Ground to space optical communication characterization", Proc. SPIE, 2005, vol. 5892, pp. 589202-1– 589202-16.
- [5] Sodnik Z, Furch B, Lutz H., "The ESA Optical Ground Station – Ten Years Since First Light", ESA bulletin 132, November 2007, pp. 34 – 40.
- [6] Toyoshima M., Yamakawa S., Yamawaki T., Arai K., Reyes M., Alonso A., Sodnik Z., Demelenne B., "Ground-to-satellite optical link tests between the Japanese laser communication terminal and the European geostationary satellite ARTEMIS", Proc. SPIE, 2004, vol. 5338A.
- [7] Toyoshima M, Yamakawa S, Yamawaki T, Arai K, Reyes M, Alonso A, Sodnik Z, and Demelenne B, "Long-term statistics of laser beam propagation in an optical ground-to-geostationary satellite communications link," IEEE Trans. on Antennas and Propagation, 2005, vol. 53, no. 2, pp. 842–850.
- [8] T. Jono, Y. Takayama, N. Kura, K. Ohinata, Y. Koyama, K. Shiratama, Z. Sodnik, B. Demelenne, A. Bird, and K. Arai, "OICETS on-orbit laser communication experiments," Proc. SPIE, 2006, vol. 6105, pp. 13–23.
- [9] Lange R., Smutny B., "Homodyne BPSK-based optical inter-satellite communication links", Proc. SPIE, 2007, Vol. 6457, p. 645703.
- [10] K.-J. Schulz, J. Rush et al., "Optical Link Study Group Final Report," IOAG-15b, June 2012.
- [11] B. Hine, S. Spremo, M. Turner, R. Caffrey, "The Lunar Atmosphere and Dust Environment Explorer (LADEE) Mission," 20100021423, June 2010.
- [12] B.S. Robinson, D.M. Boroson, D.A. Burianek, D.V. Murphy, "The Lunar Laser Communications Demonstration," Space Optical Systems and Applications (ICSOS), 2011 International Conference on , pp.54-57, 11-13 May 2011.
- [13] M. E. Grein, et al., "Design of a Ground-Based Optical Receiver for the Lunar Laser Communications Demonstration," Space Optical Systems and Applications (ICSOS), 2011 International Conference on , pp.78-82, 11-13 May 2011.
- [14] LLCD Lunar Lasercom Space Terminal (LLST) to Co-operating Ground Terminal (CGT) Interface Control Document, LLCD-CGT-ICD-001, Goddard Space Flight Center.
- [15] Arnold F., Mosberger M., Widmer J. and Gambarara F., "Ground receiver unit for optical communication between LADEE spacecraft and ESA ground station", SPIE, 2014, vol. 8971
- [16] Sans M., Sodnik Z., Zayer I. and Daddato R., "Design of ESA's Optical Ground Station for Participation in LLCD", Proc. ICSOS 2012, Ajaccio
- [17] Sodnik Z., Smit H., Sans M., Zayer I., Lanucara M., Montilla I., Alonso A. "LLCD Operations using the Lunar Lasercom OGS Terminal", SPIE, 2014, vol. 8971